

Multiplicity and Pseudorapidity Distributions of Photons in Au + Au Collisions at $\sqrt{s_{NN}} = 62.4$ GeV

J. Adams,³ M. M. Aggarwal,²⁹ Z. Ahammed,⁴³ J. Amonett,²⁰ B. D. Anderson,²⁰ D. Arkhipkin,¹³ G. S. Averichev,¹² S. K. Badyal,¹⁹ Y. Bai,²⁷ J. Balewski,¹⁷ O. Barannikova,³² L. S. Barnby,³ J. Baudot,¹⁸ S. Bekele,²⁸ V. V. Belaga,¹² A. Bellingeri-Laurikainen,³⁸ R. Bellwied,⁴⁶ J. Berger,¹⁴ B. I. Bezverkhny,⁴⁸ S. Bhardwaj,³³ A. Bhasin,¹⁹ A. K. Bhati,²⁹ H. Bichsel,⁴⁵ J. Bielcik,⁴⁸ J. Bielcikova,⁴⁸ A. Billmeier,⁴⁶ L. C. Bland,⁴ C. O. Blyth,³ S. Blyth,²¹ B. E. Bonner,³⁴ M. Botje,²⁷ A. Boucham,³⁸ J. Bouchet,³⁸ A. V. Brandin,²⁵ A. Bravar,⁴ M. Bystersky,¹¹ R. V. Cadman,¹ X. Z. Cai,³⁷ H. Caines,⁴⁸ M. Calderón de la Barca Sánchez,¹⁷ J. Castillo,²¹ O. Catu,⁴⁸ D. Cebra,⁷ Z. Chajecski,⁴⁴ P. Chaloupka,¹¹ S. Chattopadhyay,⁴³ H. F. Chen,³⁶ Y. Chen,⁸ J. Cheng,⁴¹ M. Cherney,¹⁰ A. Chikhanian,⁴⁸ W. Christie,⁴ J. P. Coffin,¹⁸ T. M. Cormier,⁴⁶ M. R. Cosentino,³⁵ J. G. Cramer,⁴⁵ H. J. Crawford,⁶ D. Das,⁴³ S. Das,⁴³ M. M. de Moura,³⁵ T. G. Dedovich,¹² A. A. Derevschikov,³¹ L. Didenko,⁴ T. Dietel,¹⁴ S. M. Dogra,¹⁹ W. J. Dong,⁸ X. Dong,³⁶ J. E. Draper,⁷ F. Du,⁴⁸ A. K. Dubey,¹⁵ V. B. Dunin,¹² J. C. Dunlop,⁴ M. R. Dutta Mazumdar,⁴³ V. Eckardt,²³ W. R. Edwards,²¹ L. G. Efimov,¹² V. Emelianov,²⁵ J. Engelage,⁶ G. Eppley,³⁴ B. Erazmus,³⁸ M. Estienne,³⁸ P. Fachini,⁴ J. Faivre,¹⁸ R. Fatemi,¹⁷ J. Fedorisin,¹² K. Filimonov,²¹ P. Filip,¹¹ E. Finch,⁴⁸ V. Fine,⁴ Y. Fisyak,⁴ K. S. F. Fornazier,³⁵ J. Fu,⁴¹ C. A. Gagliardi,³⁹ L. Gaillard,³ J. Gans,⁴⁸ M. S. Ganti,⁴³ F. Geurts,³⁴ V. Ghazikhanian,⁸ P. Ghosh,⁴³ J. E. Gonzalez,⁸ H. Gos,⁴⁴ O. Grachov,⁴⁶ O. Grebenyuk,²⁷ D. Grosnick,⁴² S. M. Guertin,⁸ Y. Guo,⁴⁶ A. Gupta,¹⁹ T. D. Gutierrez,⁷ T. J. Hallman,⁴ A. Hamed,⁴⁶ D. Hardtke,²¹ J. W. Harris,⁴⁸ M. Heinz,² T. W. Henry,³⁹ S. Hepplemann,³⁰ B. Hippolyte,¹⁸ A. Hirsch,³² E. Hjort,²¹ G. W. Hoffmann,⁴⁰ M. Horner,²¹ H. Z. Huang,⁸ S. L. Huang,³⁶ E. W. Hughes,⁵ T. J. Humanic,²⁸ G. Igo,⁸ A. Ishihara,⁴⁰ P. Jacobs,²¹ W. W. Jacobs,¹⁷ M. Jedynak,⁴⁴ H. Jiang,⁸ P. G. Jones,³ E. G. Judd,⁶ S. Kabana,² K. Kang,⁴¹ M. Kaplan,⁹ D. Keane,²⁰ A. Kechechyan,¹² V. Yu. Khodyrev,³¹ J. Kiryluk,²² A. Kisiel,⁴⁴ E. M. Kislov,¹² J. Klay,²¹ S. R. Klein,²¹ D. D. Koetke,⁴² T. Kollegger,¹⁴ M. Kopytine,²⁰ L. Kotchenda,²⁵ K. L. Kowalik,²¹ M. Kramer,²⁶ P. Kravtsov,²⁵ V. I. Kravtsov,³¹ K. Krueger,¹ C. Kuhn,¹⁸ A. I. Kulikov,¹² A. Kumar,²⁹ R. Kh. Kutuev,¹³ A. A. Kuznetsov,¹² M. A. C. Lamont,⁴⁸ J. M. Landgraf,⁴ S. Lange,¹⁴ F. Laue,⁴ J. Lauret,⁴ A. Lebedev,⁴ R. Lednický,¹² S. Lehocka,¹² M. J. LeVine,⁴ C. Li,³⁶ Q. Li,⁴⁶ Y. Li,⁴¹ G. Lin,⁴⁸ S. J. Lindenbaum,²⁶ M. A. Lisa,²⁸ F. Liu,⁴⁷ H. Liu,³⁶ J. Liu,³⁴ L. Liu,⁴⁷ Q. J. Liu,⁴⁵ Z. Liu,⁴⁷ T. Ljubicic,⁴ W. J. Llope,³⁴ H. Long,⁸ R. S. Longacre,⁴ M. Lopez-Noriega,²⁸ W. A. Love,⁴ Y. Lu,⁴⁷ T. Ludlam,⁴ D. Lynn,⁴ G. L. Ma,³⁷ J. G. Ma,⁸ Y. G. Ma,³⁷ D. Magestro,²⁸ S. Mahajan,¹⁹ D. P. Mahapatra,¹⁵ R. Majka,⁴⁸ L. K. Mangotra,¹⁹ R. Manweiler,⁴² S. Margetis,²⁰ C. Markert,²⁰ L. Martin,³⁸ J. N. Marx,²¹ H. S. Matis,²¹ Yu. A. Matulenko,³¹ C. J. McClain,¹ T. S. McShane,¹⁰ F. Meissner,²¹ Yu. Melnick,³¹ A. Meschanin,³¹ M. L. Miller,²² N. G. Minaev,³¹ C. Mironov,²⁰ A. Mischke,²⁷ D. K. Mishra,¹⁵ J. Mitchell,³⁴ B. Mohanty,⁴³ L. Molnar,³² C. F. Moore,⁴⁰ D. A. Morozov,³¹ M. G. Munhoz,³⁵ B. K. Nandi,¹⁶ S. K. Nayak,¹⁹ T. K. Nayak,⁴³ J. M. Nelson,³ P. K. Netrakanti,⁴³ V. A. Nikitin,¹³ L. V. Nogach,³¹ S. B. Nurushev,³¹ G. Odyniec,²¹ A. Ogawa,⁴ V. Okorokov,²⁵ M. Oldenburg,²¹ D. Olson,²¹ S. K. Pal,⁴³ Y. Panebratsev,¹² S. Y. Panitkin,⁴ A. I. Pavlinov,⁴⁶ T. Pawlak,⁴⁴ T. Peitzmann,²⁷ V. Perevoztchikov,⁴ C. Perkins,⁶ W. Peryt,⁴⁴ V. A. Petrov,¹³ S. C. Phatak,¹⁵ R. Picha,⁷ M. Planinic,⁴⁹ J. Pluta,⁴⁴ N. Porile,³² J. Porter,⁴⁵ A. M. Poskanzer,²¹ M. Potekhin,⁴ E. Potrebenikova,¹² B. V. K. S. Potukuchi,¹⁹ D. Prindle,⁴⁵ C. Pruneau,⁴⁶ J. Putschke,²³ G. Rakness,³⁰ R. Raniwala,³³ S. Raniwala,³³ O. Ravel,³⁸ R. L. Ray,⁴⁰ S. V. Razin,¹² D. Reichhold,³² J. G. Reid,⁴⁵ J. Reinrath,³⁸ G. Renault,³⁸ F. Retiere,²¹ A. Ridiger,²⁵ H. G. Ritter,²¹ J. B. Roberts,³⁴ O. V. Rogachevskiy,¹² J. L. Romero,⁷ A. Rose,⁴⁶ C. Roy,³⁸ L. Ruan,³⁶ M. J. Russcher,⁵⁰ R. Sahoo,¹⁵ I. Sakrejda,²¹ S. Salur,⁴⁸ J. Sandweiss,⁴⁸ M. Sarsour,¹⁷ I. Savin,¹³ P. S. Sazhin,¹² J. Schambach,⁴⁰ R. P. Scharenberg,³² N. Schmitz,²³ K. Schweda,²¹ J. Seger,¹⁰ P. Seyboth,²³ E. Shahaliev,¹² M. Shao,³⁶ W. Shao,⁵ M. Sharma,²⁹ W. Q. Shen,³⁷ K. E. Shestermanov,³¹ S. S. Shimanskiy,¹² E. Sichtermann,²¹ F. Simon,²³ R. N. Singaraju,⁴³ N. Smirnov,⁴⁸ R. Snellings,²⁷ G. Sood,⁴² P. Sorensen,²¹ J. Sowinski,¹⁷ J. Speltz,¹⁸ H. M. Spinka,¹ B. Srivastava,³² A. Stadnik,¹² T. D. S. Stanislaus,⁴² R. Stock,¹⁴ A. Stolpovsky,⁴⁶ M. Strikhanov,²⁵ B. Stringfellow,³² A. A. P. Suaide,³⁵ E. Sugarbaker,²⁸ C. Suire,⁴ M. Sumera,¹¹ B. Surrow,²² M. Swanger,¹⁰ T. J. M. Symons,²¹ A. Szanto de Toledo,³⁵ A. Tai,⁸ J. Takahashi,³⁵ A. H. Tang,²⁷ T. Tarnowsky,³² D. Thein,⁸ J. H. Thomas,²¹ S. Timoshenko,²⁵ M. Tokarev,¹² T. A. Trainor,⁴⁵ S. Trentalange,⁸ R. E. Tribble,³⁹ O. D. Tsai,⁸ J. Ulery,³² T. Ullrich,⁴ D. G. Underwood,¹ G. Van Buren,⁴ M. van Leeuwen,²¹ A. M. Vander Molen,²⁴ R. Varma,¹⁶ I. M. Vasilevski,¹³ A. N. Vasiliev,³¹ R. Vernet,¹⁸ S. E. Vigdor,¹⁷ Y. P. Viyogi,⁴³ S. Vokal,¹² S. A. Voloshin,⁴⁶ W. T. Waggoner,¹⁰ F. Wang,³² G. Wang,²⁰ G. Wang,⁵ X. L. Wang,³⁶ Y. Wang,⁴⁰ Y. Wang,⁴¹ Z. M. Wang,³⁶ H. Ward,⁴⁰ J. W. Watson,²⁰ J. C. Webb,¹⁷ G. D. Westfall,²⁴ A. Wetzler,²¹ C. Whitten, Jr.,⁸ H. Wieman,²¹ S. W. Wissink,¹⁷ R. Witt,² J. Wood,⁸ J. Wu,³⁶ N. Xu,²¹ Z. Xu,⁴ Z. Z. Xu,³⁶

E. Yamamoto,²¹ P. Yepes,³⁴ V. I. Yurevich,¹² I. Zborovsky,¹¹ H. Zhang,⁴ W. M. Zhang,²⁰ Y. Zhang,³⁶ Z. P. Zhang,³⁶
R. Zoukarneev,¹³ Y. Zoukarneeva,¹³ and A. N. Zubarev¹²

(STAR Collaboration)

- ¹Argonne National Laboratory, Argonne, Illinois 60439, USA
²University of Bern, 3012 Bern, Switzerland
³University of Birmingham, Birmingham, United Kingdom
⁴Brookhaven National Laboratory, Upton, New York 11973, USA
⁵California Institute of Technology, Pasadena, California 91125, USA
⁶University of California, Berkeley, California 94720, USA
⁷University of California, Davis, California 95616, USA
⁸University of California, Los Angeles, California 90095, USA
⁹Carnegie Mellon University, Pittsburgh, Pennsylvania 15213, USA
¹⁰Creighton University, Omaha, Nebraska 68178, USA
¹¹Nuclear Physics Institute AS CR, 250 68 Řež/Prague, Czech Republic
¹²Laboratory for High Energy (JINR), Dubna, Russia
¹³Particle Physics Laboratory (JINR), Dubna, Russia
¹⁴University of Frankfurt, Frankfurt, Germany
¹⁵Institute of Physics, Bhubaneswar 751005, India
¹⁶Indian Institute of Technology, Mumbai, India
¹⁷Indiana University, Bloomington, Indiana 47408, USA
¹⁸Institut de Recherches Subatomiques, Strasbourg, France
¹⁹University of Jammu, Jammu 180001, India
²⁰Kent State University, Kent, Ohio 44242, USA
²¹Lawrence Berkeley National Laboratory, Berkeley, California 94720, USA
²²Massachusetts Institute of Technology, Cambridge, Massachusetts 02139-4307, USA
²³Max-Planck-Institut für Physik, Munich, Germany
²⁴Michigan State University, East Lansing, Michigan 48824, USA
²⁵Moscow Engineering Physics Institute, Moscow Russia
²⁶City College of New York, New York City, New York 10031, USA
²⁷NIKHEF, Amsterdam, The Netherlands
²⁸Ohio State University, Columbus, Ohio 43210, USA
²⁹Panjab University, Chandigarh 160014, India
³⁰Pennsylvania State University, University Park, Pennsylvania 16802, USA
³¹Institute of High Energy Physics, Protvino, Russia
³²Purdue University, West Lafayette, Indiana 47907, USA
³³University of Rajasthan, Jaipur 302004, India
³⁴Rice University, Houston, Texas 77251, USA
³⁵Universidade de Sao Paulo, Sao Paulo, Brazil
³⁶University of Science & Technology of China, Anhui 230027, China
³⁷Shanghai Institute of Applied Physics, Shanghai 201800, China
³⁸SUBATECH, Nantes, France
³⁹Texas A&M University, College Station, Texas 77843, USA
⁴⁰University of Texas, Austin, Texas 78712, USA
⁴¹Tsinghua University, Beijing 100084, China
⁴²Valparaiso University, Valparaiso, Indiana 46383, USA
⁴³Variable Energy Cyclotron Centre, Kolkata 700064, India
⁴⁴Warsaw University of Technology, Warsaw, Poland
⁴⁵University of Washington, Seattle, Washington 98195, USA
⁴⁶Wayne State University, Detroit, Michigan 48201, USA
⁴⁷Institute of Particle Physics, CCNU (HZNU), Wuhan 430079, China
⁴⁸Yale University, New Haven, Connecticut 06520, USA
⁴⁹University of Zagreb, Zagreb, HR-10002, Croatia
⁵⁰NIKHEF and Utrecht University, Amsterdam, The Netherlands

(Received 4 February 2005; revised manuscript received 12 April 2005; published 5 August 2005)

We present the first measurement of pseudorapidity distribution of photons in the region $2.3 \leq \eta \leq 3.7$ for different centralities in Au + Au collisions at $\sqrt{s_{NN}} = 62.4$ GeV. We find that the photon yield scales with the number of participating nucleons at all collision centralities studied. The pseudorapidity

distribution of photons, dominated by π^0 decays, has been compared to those of charged pions, photons, and inclusive charged particles from heavy-ion and nucleon-nucleon collisions at various energies. The photon production has been shown to be consistent with the energy and centrality independent limiting fragmentation scenario.

DOI: [10.1103/PhysRevLett.95.062301](https://doi.org/10.1103/PhysRevLett.95.062301)

PACS numbers: 25.75.Dw

One of the primary goals of the heavy-ion program at the Relativistic Heavy-Ion Collider (RHIC) at Brookhaven National Laboratory is to search for the possible formation of Quark-Gluon Plasma [1]. Important information about the dynamics of particle production and the evolution of the system formed in the collision can be obtained from various global observables, such as the multiplicity of photons and charged particles. At RHIC energies, the particle production mechanisms could be different in different regions of pseudorapidity (η) [2,3]. At midrapidity a significant increase in charged particle production normalized to the number of participating nucleons (N_{part}) has been observed for central Au + Au collisions compared to peripheral Au + Au and $p + p$ collisions [4]. This has been attributed to the onset of hard scattering processes, which scale with the number of binary collisions. Alternatively, in the color glass condensate [5] picture of particle production at midrapidity, the centrality dependence reflects increasing gluon density due to the decrease in the effective strong coupling constant. However, the total charged particle multiplicity per N_{part} pair, integrated over the whole η range, is independent of centrality in Au + Au collisions [2].

It is also observed that the number of charged particles produced per participant pair as a function of $\eta - y_{\text{beam}}$, where y_{beam} is the beam rapidity, is independent of beam energy [2]. This phenomenon is known as limiting fragmentation (LF) [6]. There have been contradictory results reported from inclusive charged particle measurements regarding the centrality dependence of the LF behavior, results from the PHOBOS collaboration show a centrality dependence [2], while those from the BRAHMS collaboration show a centrality independent behavior [3]. The centrality dependence at forward rapidities has been attributed to nuclear remnants, baryon stopping, and may be due to a new mechanism of baryon production [7]. Further insight into this question can be obtained by studying the centrality, beam energy, and system size dependence of LF phenomena with identified particles. Energy independence of LF for pions has been found in e^+e^- collisions [8].

Photons are produced in all stages of the system created in heavy-ion collisions. They do not interact strongly with the medium and carry information about the history of the collision. Since inclusive photon production is dominated by photons from the decay of π^0 's, measurement of the multiplicity of photons is complementary to the charged pion measurements. The forward rapidity region in heavy-ion collisions, where the present measurements have been

carried out, constitutes an environment that precludes the use of a calorimeter due to the high level of overlap of fully developed showers. The only measurements of photon multiplicity distribution in the forward rapidity region reported to date are from a preshower detector [9] at the Super Proton Synchrotron (SPS), resulting in the study of various aspects of the reaction mechanism in heavy-ion collisions [10,11].

In this Letter we present the first measurement of photon production at the forward rapidities ($2.3 \leq \eta \leq 3.7$), carried out by the STAR experiment [12] using a highly granular preshower photon multiplicity detector (PMD) [13] in Au + Au collisions at $\sqrt{s_{NN}} = 62.4$ GeV. The minimum bias trigger is obtained using the charged particle hits from an array of scintillator slats arranged in a barrel called the central trigger barrel surrounding the time projection chamber (TPC) and two zero degree hadronic calorimeters at ± 18 m from the detector center [14]. A total of 334 000 minimum bias events, corresponding to 0 to 80% of the Au + Au hadronic interaction cross section, have been selected with a collision vertex position of less than 30 cm from the center of the TPC along the beam axis. The centrality determination in this analysis uses the multiplicity of charged particles in the pseudorapidity region $|\eta| < 0.5$, as measured by the TPC [15].

The PMD is located 5.4 meters away from the center of the TPC (the nominal collision point) along the beam axis. It consists of two planes (charged particle veto and preshower) of an array of cellular gas proportional counters [13]. A lead plate of 3 r.l. thickness was placed between the two planes and was used as a photon converter. The sensitive medium is a gas mixture of Ar and CO₂ in the ratio of 70%:30% by weight. There are 41472 cells in each plane, placed inside 12 high voltage insulated and gas-tight chambers called super modules (SMs). A photon traversing the converter produces an electromagnetic shower in the preshower plane, leading to a larger signal spread over several cells as compared to a charged particle which is essentially confined to one cell [13]. The present analysis uses data from the preshower plane only.

The cellwise response is obtained by using the ADC distributions of isolated cells. The ADC distribution of an isolated cell may be treated as the response of the cell to charged particles [13]. For most of the cells this response followed a Landau distribution. We used the mean of the ADC distribution of isolated cells to estimate and correct the relative gains of all cells within each SM. The cell-to-cell gain variation within a SM varied between 10–25% for different SMs.

The extraction of photon multiplicity proceeds in two steps involving clustering of hits and photon-hadron discrimination. Hit clusters consist of contiguous cells. Photons are separated from charged particles using the following conditions based on Monte Carlo simulations: (a) The number of cells in a cluster is >1 and (b) the cluster signal is larger than 3 times the average response of all isolated cells in a SM. The number of selected clusters, called γ -like clusters ($N_{\gamma\text{-like}}$), in different SMs for the same η coverage is used to evaluate the effect of possible nonuniformity in the response of the detector.

To estimate the number of photons (N_γ) from the detected $N_{\gamma\text{-like}}$ clusters we evaluate the photon reconstruction efficiency (ϵ_γ) and purity (f_p) of the γ -like sample defined [10] as $\epsilon_\gamma = N_{\text{cls}}^{\gamma,\text{th}}/N_\gamma$ and $f_p = N_{\text{cls}}^{\gamma,\text{th}}/N_{\gamma\text{-like}}$ respectively. $N_{\text{cls}}^{\gamma,\text{th}}$ is the number of photon clusters after the photon-hadron discrimination conditions. Both ϵ_γ and f_p are obtained from a detailed Monte Carlo simulation using the HIJING event generator (version 1.382) [16] with default parameter settings and the detector simulation package GEANT [17]. The lower limit of photon p_T acceptance in the PMD is estimated to be 20 MeV/c. Both ϵ_γ and f_p vary with η and centrality due to variations in particle density, upstream conversions, and detector related effects. The highest occupancy is $\sim 12\%$ and the maximum percentage of split cluster is 9%. The ϵ_γ value is found to increase from 42% to 56% in central collisions and from 42% to 70% in peripheral collisions as η increases from 2.3 to 3.7. The f_p value sample ranges from 55% to 62%, and from 63% to 70% for central and peripheral collisions, respectively, as we increase η within the above range.

The systematic errors on the photon multiplicity (N_γ) are due to (a) uncertainty in estimates of ϵ_γ and f_p values, arising from splitting of clusters and the choice of photon-hadron discrimination conditions and (b) uncertainty in N_γ arising from the nonuniformity of the detector primarily due to cell-to-cell gain variation. The error in N_γ due to (a) is estimated from Monte Carlo simulations to be 9.8% and 7.7% in central and peripheral collisions, respectively. The error in N_γ due to (b) is estimated using average gains for normalization and by studying the azimuthal dependence of photon density of the detector in a η window. This is found to be 13.5% for central and 15% for peripheral collisions. The total systematic error in N_γ is $\sim 17\%$ for both central and peripheral collisions. The systematic and statistical errors added in quadrature are shown in all the figures.

Figure 1 shows the minimum bias distribution of N_γ along with results from *HIJING + GEANT* and a multiphase transport model (AMPT) [18] models. The HIJING model is based on perturbative QCD processes which lead to multiple jet production and jet interactions in matter. The AMPT model is a multiphase transport model which includes both initial partonic and final hadronic interactions. We observe that HIJING underpredicts the measured N_γ

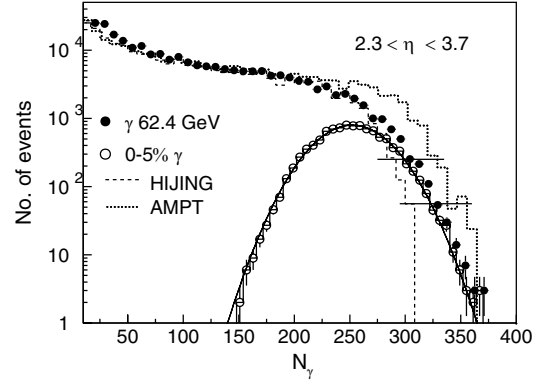


FIG. 1. Minimum bias N_γ distribution. Comparison with HIJING and AMPT models are shown. Horizontal bars indicate the errors. The N_γ distribution for top 5% central events is shown in open circles. The solid curve is a fit by a Gaussian function.

whereas AMPT slightly overpredicts the total measured N_γ for central collisions. Within the errors, the two models are in agreement with the measurement. The top 5% central N_γ distribution (open circles) is fitted by a Gaussian function with a mean of 252.

Figure 2 shows the pseudorapidity distribution of photons for various event centrality classes. The results from HIJING are systematically lower compared to data for mid-central and peripheral events. The results from AMPT compare well with the data.

Figure 3 shows the variation of total number of photons per participant pair in the PMD coverage as a function of the number of participants. N_{part} is obtained from Glauber calculations [15]. Higher values of N_{part} corresponds to central collisions. We observe that the N_γ per N_{part} pair is approximately constant with centrality. The values from HIJING are lower compared to the data. The values from AMPT agree fairly well with those obtained from the data. Approximate linear scaling of N_γ with N_{part} in the η range studied indicates that photon production is consistent with

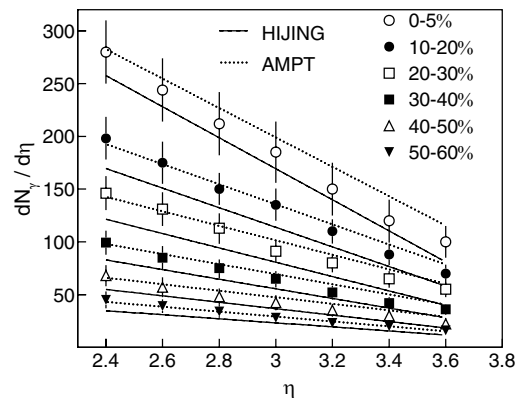


FIG. 2. $\frac{dN_\gamma}{d\eta}$ for various event centrality classes compared to HIJING and AMPT model calculations.

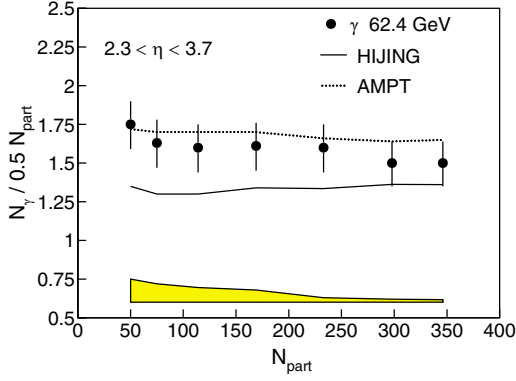


FIG. 3 (color online). Variation of N_γ per participant pair in PMD coverage ($2.3 \leq \eta \leq 3.7$) as a function of N_{part} . The lower band reflects uncertainties in N_{part} calculations.

nucleus-nucleus collisions being a superposition of nucleon-nucleon collisions.

In Fig. 4 we present the energy and centrality dependence of LF for inclusive photons and charged particles. Figure 4(a) compares the $\frac{dN_\gamma}{d\eta}$ distributions for central (0–5%) and peripheral (40–50%) Au + Au collisions at $\sqrt{s_{NN}} = 62.4$ GeV, with the top SPS energy central (0–5%) photon data for Pb + Pb collisions [10] as a function of $\eta - y_{\text{beam}}$. Also shown is the $\frac{dN_\gamma}{d\eta}$ from $p\bar{p}$ collisions at $\sqrt{s_{NN}} = 540$ GeV [19]. In Fig. 4(b) we show the $\frac{dN_{\text{ch}}}{d\eta}$ distributions for central (0–6%), peripheral (35–40%) Au + Au collisions at $\sqrt{s_{NN}} = 200$ GeV and central data at $\sqrt{s_{NN}} = 130$ GeV from the PHOBOS [2] and BRAHMS

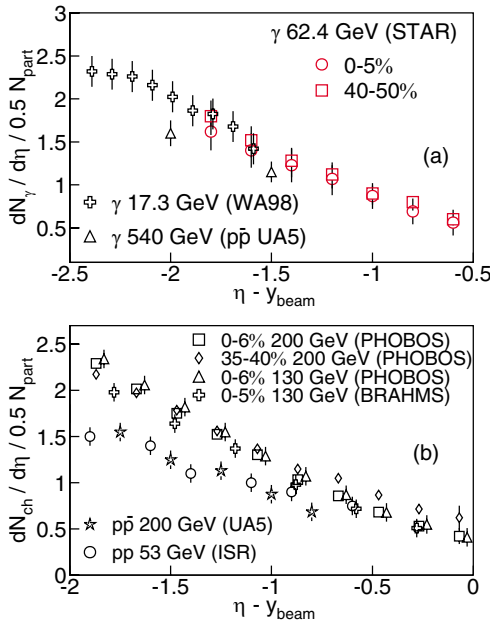


FIG. 4 (color online). (a) Variation of $\frac{dN_\gamma}{d\eta}$ normalized to N_{part} with $\eta - y_{\text{beam}}$ for different collision energy and centrality. Also shown $\frac{dN_\gamma}{d\eta}$ for $p\bar{p}$ collisions. (b) same as (a) for charged particles.

[3] collaborations as a function of $\eta - y_{\text{beam}}$. Also shown are the $\frac{dN_{\text{ch}}}{d\eta}$ from pp and $p\bar{p}$ collisions at $\sqrt{s_{NN}} = 53$ and 200 GeV [19]. We observe in Fig. 4(a) that photon results from the SPS and RHIC are consistent with each other, suggesting that photon production follows an energy independent LF behavior. Energy independent LF behavior for charged particles can be seen in Fig. 4(b) from the comparison of $\frac{dN_{\text{ch}}}{d\eta}$ from the PHOBOS collaboration for $\sqrt{s_{NN}} = 130$ and 200 GeV and the BRAHMS collaboration at $\sqrt{s_{NN}} = 130$ GeV [2,3].

In Fig. 4(a) we also observe that $\frac{dN_\gamma}{d\eta}$ as a function of $\eta - y_{\text{beam}}$ is independent of centrality. However, in Fig. 4(b) it is observed that $\frac{dN_{\text{ch}}}{d\eta}$ as a function of $\eta - y_{\text{beam}}$ is dependent on centrality [2]. The centrality dependence has been speculated to be due to nuclear remnants and baryon stopping [2,7]. The dependence of LF on the collision system is most clearly seen in the comparison between results from heavy-ion collisions with those from pp and $p\bar{p}$ collisions. We observe in Fig. 4(a) that the photon results in the forward rapidity region from $p\bar{p}$ collisions at $\sqrt{s_{NN}} = 540$ GeV are in close agreement with the measured photon yield in Au + Au collisions at $\sqrt{s_{NN}} = 62.4$ GeV. However the pp and $p\bar{p}$ inclusive charged particle results are very different from those reported by the PHOBOS collaboration [Fig. 4(b)]. This indicates that there is apparently a significant charged baryon contribution in nucleus-nucleus collisions at the forward η region.

Figure 5 shows the charged pion rapidity density in Au + Au collisions RHIC [20] and Pb + Pb collisions at the SPS [21] and estimated $\frac{dN_{\pi^0}}{dy}$ from the present measurement ($\frac{dN_\gamma}{dy}$) at $\sqrt{s_{NN}} = 62.4$ GeV, all as a function of $y - y_{\text{beam}}$. HIJING calculations indicate that about 93–96% of photons are from π^0 decays. From HIJING we obtained the ratio of the photon to π^0 yields. This ratio is used to estimate the π^0 yield from the measured photon yield.

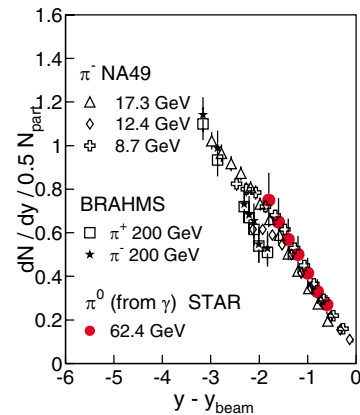


FIG. 5 (color online). Estimated $\frac{dN_{\pi^0}}{dy}$ from $\frac{dN_\gamma}{dy}$ normalized to N_{part} , as compared to $\frac{dN_{\pi^\pm}}{dy}$ normalized to N_{part} , as a function of $y - y_{\text{beam}}$ for central collisions at various collision energies.

The BRAHMS collaboration results at forward rapidities are slightly lower compared to the results from SPS energies. However, in general, the results show that pion production in heavy-ion collisions in the fragmentation region agrees with the LF picture. Similar features have been observed in e^+e^- collisions [8]. The centrality dependence of LF for inclusive charged hadrons and the centrality independence of LF for identified mesons indicate that although the baryon stopping is different in different collision systems, the pions produced at forward rapidities are not affected by the baryon transport.

In summary, we have presented the first results of photon multiplicity measurements at RHIC in the pseudorapidity region $2.3 \leq \eta \leq 3.7$. The pseudorapidity distributions of photons have been obtained for various centrality classes. Photon production per participant pair is found to be approximately independent of centrality in this η region. Comparison with photon and charged pion data at RHIC and SPS energies shows, for the first time in heavy-ion collisions, that photons and pions follow an energy independent limiting fragmentation behavior, as previously found for inclusive charged particles. Furthermore, photons are observed to follow a centrality independent limiting fragmentation scenario.

We thank the RHIC Operations Group and RCF at BNL, and the NERSC Center at LBNL for their support. This work was supported in part by the HENP Divisions of the Office of Science of the U.S. DOE; the U.S. NSF; the BMBF of Germany; IN2P3, RA, RPL, and EMN of France; EPSRC of the United Kingdom; FAPESP of Brazil; the Russian Ministry of Science and Technology; the Ministry of Education and the NNSFC of China; SFOM of the Czech Republic, FOM and UU of the Netherlands, DAE, DST, and CSIR of the government of India; the Swiss NSF; the Polish State Committee for Scientific Research; STAA of Slovakia, and the Korea Science and Engineering Foundation. We acknowledge the help of CERN for use of GASSIPLEX chips in the PMD readout.

[1] *Proceedings of Quark Matter 2004* [Jour. of Phys. G 30 (2004)].

- [2] B.B. Back *et al.* (PHOBOS Collaboration), Phys. Rev. Lett. **87**, 102303 (2001); Phys. Rev. Lett. **91**, 052303 (2003); Nucl. Phys. **A757**, 28 (2005).
- [3] I.G. Bearden *et al.* (BRAHMS Collaboration), Phys. Lett. B **523**, 227 (2001); Phys. Rev. Lett. **88**, 202301 (2002).
- [4] K. Adcox *et al.* (PHENIX Collaboration), Phys. Rev. Lett. **86**, 3500 (2001).
- [5] D. Kharzeev and Marzia Nardi, Phys. Lett. B **507**, 121 (2001); E. Iancu, A. Leonidov, and L. McLerran, hep-ph/0202270.
- [6] J. Benecke *et al.*, Phys. Rev. **188**, 2159 (1969).
- [7] D. Kharzeev, Phys. Lett. B **378**, 238 (1996); V. Topor Pop *et al.*, Phys. Rev. C **70**, 064906 (2004).
- [8] D.E. Groom *et al.*, Eur. Phys. J. C **15**, 227 (2000); H. Albrecht *et al.*, Z. Phys. C **44**, 547 (1989); H. Aihara *et al.*, Phys. Rev. Lett. **61**, 1263 (1988); D. Buskulic *et al.*, Z. Phys. C **66**, 355 (1995).
- [9] M. M. Aggarwal *et al.*, Nucl. Instrum. Methods Phys. Res., Sect. A **372**, 143 (1996); Nucl. Instrum. Methods Phys. Res., Sect. A **424**, 395 (1999).
- [10] M. M. Aggarwal *et al.* (WA98 Collaboration), Phys. Lett. B **458**, 422 (1999); Phys. Rev. C **64**, 011901(R) (2001).
- [11] M. M. Aggarwal *et al.* (WA93 Collaboration), Phys. Rev. C **58**, 1146 (1998); Phys. Lett. B **403**, 390 (1997).
- [12] K. H. Ackermann *et al.*, Nucl. Instrum. Methods Phys. Res., Sect. A **499**, 624 (2003).
- [13] M. M. Aggarwal *et al.*, Nucl. Instrum. Methods Phys. Res., Sect. A **499**, 751 (2003); Nucl. Instrum. Methods Phys. Res., Sect. A **488**, 131 (2002).
- [14] F. S. Bieser *et al.*, Nucl. Instrum. Methods Phys. Res., Sect. A **499**, 766 (2003).
- [15] J. Adams *et al.* (STAR Collaboration), nucl-ex/0311017.
- [16] X.-N. Wang and M. Gyulassy, Phys. Rev. D **44**, 3501 (1991).
- [17] V. Fine and P. Nevski, in *Proceedings of CHEP-2000, Padova, Italy* (to be published).
- [18] B. Zhang *et al.*, Phys. Rev. C **61**, 067901 (2000).
- [19] K. Alpgard *et al.* (UA5 Collaboration), Phys. Lett. B **115**, 71 (1982); G.J. Alner *et al.*, Z. Phys. C **33**, 1 (1986).
- [20] I. G. Bearden *et al.* (BRAHMS Collaboration), Phys. Rev. Lett. **94**, 162301 (2005).
- [21] S. V. Afanasiev *et al.* (NA49 Collaboration), Phys. Rev. C **66**, 054902 (2002).